IEEE Photonics Journal
An IEEE Photonics Society Publication

Open Access

Broadband and High Extinction Ratio Mode Converter Using the Tapered Hybrid Plasmonic Waveguide

Volume 11, Number 3, June 2019

Zhuo Cheng
Jun Wang
Zeyuan Yang
Haiying Yin
Wei Wang
Yongqing Huang
Xiaomin Ren

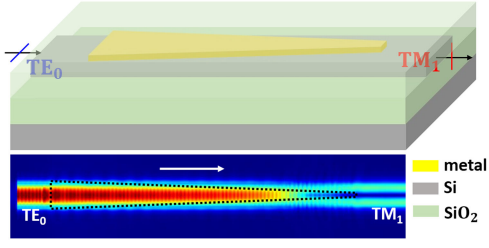

DOI: 10.1109/JPHOT.2019.2919588
1943-0655 © 2019 IEEE

IEEE photonics SOCIETY

IEEE

Broadband and High Extinction Ratio Mode Converter Using the Tapered Hybrid Plasmonic Waveguide

Zhuo Cheng, Jun Wang, Zeyuan Yang, Haiying Yin, Wei Wang, Yongqing Huang, and Xiaomin Ren

State Key Laboratory of Information Photonics and Optical Communications, Beijing University of Posts and Telecommunications, Beijing 10086, China

DOI:10.1109/JPHOT.2019.2919588

Manuscript received May 7, 2019; revised May 23, 2019; accepted May 24, 2019. Date of publication May 28, 2019; date of current version June 11, 2019. This work was supported in part by the BUPT Excellent Ph.D. Students Foundation under Grant CX2019316; in part by the Natural National Science Foundation of China under Grant 61874148, Grant 61674020, and Grant 61574019; in part by the Beijing Natural Science Foundation under Grant 4192043; in part by the State key Laboratory of Information Photonics and Optical Communications, Beijing University of Posts and Telecommunications under Grant IPOC2018ZT01; and in part by the 111 Project of China under Grant B07005. Corresponding author: Jun Wang (e-mail: wangjun12@bupt.edu.cn).

Abstract: We propose and numerically analyze a broadband and high extinction ratio mode converter to achieve the mode conversion between the fundamental transverse electric mode (TE_0) and the first-order transverse magnetic mode (TM_1). The mode converter is achieved by using the tapered hybrid plasmonic waveguide which the metal is directly covered on the Si waveguide without a thin low-index layer. After optimizing the structure of the tapered hybrid plasmonic waveguide, a wide operation bandwidth of 100 nm is obtained with the extinction ratio of the TM_1 mode and TE_0 mode larger than 20 dB in the output Si waveguide for the forward propagation. And for the back propagation, the operation bandwidth over 65 nm is obtained with the extinction ratio larger than 20 dB in the output Si waveguide. The whole footprint of the mode converter is only $0.8 \times 11\ \mu m^2$. Fabrication tolerance analysis is also demonstrated.

Index Terms: Mode converter, hybrid plasmonic waveguide, TE_0-to-TM_1.

1. Introduction

Silicon photonics have demonstrated the great potential in meeting the growing demands for the information transmission capacity, especially in the data centers and next generation communication networks [1]–[3]. As a novel way to improve the data transmission capacity in the photonic integrated circuits (PICs), mode division multiplexing (MDM) technology which can encode the separate data for each channel provided by the different spatial eigenmodes in the waveguide and multiplex the data in the multimode waveguide has attracted more and more attentions [4], [5]. Mode converter is a key component in the MDM systems and it can manipulate the mode conversion between the different spatial eigenmodes [6]. Moreover, benefitting from the advanced fabrication technology which is compatible with the complementary metal-oxide-semiconductor (CMOS) process, the mode converter based on the silicon-on-insulator (SOI) platform has demonstrated many advantages in small footprint, easily design and low cost.

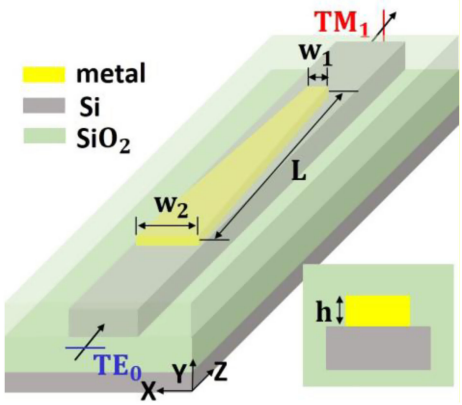

Fig. 1. Schematic diagram of the mode converter on SOI substrates.

Until now, many mode conversion devices have been demonstrated. The mode converter designed with different structures can be divided into the following categories according to the modes: (1) Conversion between the fundamental transverse mode with different polarization (such as TE_0-to-TM_0, TM_0-to-TE_0) [7]–[9]. This conversion is also called the polarization rotation. For this category mode conversion, it is usually realized by the asymmetric cross section of the waveguide and the asymmetric coupler [10], [11]. Especially, the hybrid plasmonic waveguide (HPW) with an asymmetric structure has been designed to realize the mode conversion [12]–[14]. (2) Conversion between the fundamental transverse mode and the high-order transverse mode with the same polarization (such as TE_0-to-TE_1, TE_0-to-TE_2) [15]–[17]. This conversion is also called the mode-order conversion. The second category conversion has been reported with many different structures, such as the metasurface, photonic crystal and Mach-Zender interference [18]–[20]. The basic method of the conversion includes the phase matching, beam shaping and coherent scattering. (3) Conversion between the fundamental transverse mode and the high-order transverse mode with different polarization (such as TM_0-to-TE_1, TE_0-to-TM_1) [21]–[23]. The third category conversion, however, has been less reported. In 2011, Dai *et al.* reported a tapered waveguide structure to realize the mode conversion from the TM_0 mode to the TE_1 mode [24]. The waveguide is used with the air cladding to break the vertical symmetry. The mode hybridization is appeared when the waveguide width is widen which leads to the mode conversion. Up to now, the most schemes for the TM_0-to-TE_1 conversion are based on this tapered structure with different ways to break the vertical symmetry. But for the TE_0-to-TM_1 conversion, the mode hybridization is hard to happen in the dielectric Si waveguide which the effective index of the TE_0 mode is far larger than that of the TM_1 mode. To our knowledge, there is no suitable scheme at present.

In this paper, we propose a mode converter to realize the TE_0-to-TM_1 conversion with the large operation bandwidth and the high extinction ratio. The mode converter is based on the tapered hybrid plasmonic waveguide without a thin low-index layer. The whole length of the device is about 11 μm. The proposed mode converter can be supplied to the on-chip MDM systems of the PICs.

2. Structure and Design

For a hybrid plasmonic waveguide, a thin low-index layer is usually sandwiched between the Si waveguide and the metal. But the existence of the thin low-index layer will weaken the interaction between the input TE_0 mode light and the metal, and the mode conversion even can't be achieved. So here the hybrid plasmonic waveguide used only consists of a tapered metal layer on the Si waveguide and the hybrid plasmonic waveguide is surrounded by SiO_2 cladding, the schematic diagram of the hybrid plasmonic waveguide is shown in Fig. 1. The inset is the cross section of the tapered hybrid plasmonic waveguide. The geometric parameters w_1, w_2, h and L are used to describe the metal structure. The thickness and width of the Si waveguide are decided as 340 nm

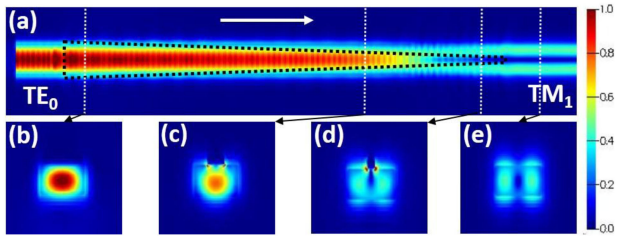

Fig. 2. (a) The electric field distributions in the hybrid plasmonic waveguide with the TE_0 mode input in the forward direction (the black dot frame indicates the metal). (b)–(e) The electric field distributions in the cross section at the corresponding positions (white dot lines).

and 0.8 μm. The refractive indexes of Si and SiO_2 are set as 3.47 and 1.44 at the wavelength of 1.55 μm [25]. As an example, the metal Au is chosen to analyze and the refractive index is $0.559 + 9.81i$ at the wavelength of 1.55 μm [25]. A finite-difference time-domain (FDTD) method is used to calculation and the mesh are set as $\Delta x = \Delta y = \Delta z = 0.01$ μm. For the forward propagation, the TE_0 mode is input from the wide metal end and converted into the TM_1 mode. For the back propagation, the TM_1 mode is input from the narrow metal end and converted into the TE_0 mode.

To further understand the process of the mode conversion, Fig. 2(a) displays the electric field distributions in the hybrid plasmonic waveguide for the forward propagation. As the width of the metal narrows, it can be found that the input TE_0 mode is gradually converted into the TM_1 mode. Through the electric field distributions in the cross section at the corresponding positions shown in Fig. 2(b)–(e), the input TE_0 mode in the dielectric waveguide (DW) is firstly coupled into the TE_0 mode in the hybrid plasmonic waveguide (see Fig. 2(b)), then due to the tip effect of the two corners between the metal and the Si waveguide, it begins to become the hybrid mode (see Fig. 2(c)). Next it is further converted into the hybrid mode which is similar to the TM_1 mode near the end of the metal (see Fig. 2(d)). Finally it is coupled out as the TM_1 mode in the dielectric Si waveguide (see Fig. 2(e)). In the process of the mode conversion, the metal absorption loss and the reflection loss are the main loss affecting the device performances. To improve the mode conversion efficiency, the geometric parameters of the metal should be optimized.

To reduce the reflection loss, the input TE_0 mode in the dielectric Si waveguide should be coupled into the TE_0 mode in the hybrid plasmonic waveguide as far as possible. Here, the power coupling ratio η is used to describe the power coupling between the TE_0 mode in the dielectric Si waveguide and the TE_0 mode in the hybrid plasmonic waveguide. The power coupling ratio is defined as follows [26]:

$$\eta = \frac{\int\int(\vec{E}_{DW} \times \vec{H}^*_{HPW} + \vec{E}^*_{HPW} \times \vec{H}_{DW})dxdy}{\int\int(\vec{E}_{DW} \times \vec{H}^*_{DW} + \vec{E}^*_{DW} \times \vec{H}_{DW})dxdy}. \tag{1}$$

Where E_{DW}, H_{DW} are the mode profiles in the dielectric Si waveguide and E_{HPW}, H_{HPW} are the mode profiles in the hybrid plasmonic waveguide. The mode profiles for the TE_0 mode in the dielectric Si waveguide and the hybrid plasmonic waveguide can be obtained by using the finite difference eigenmode (FDE) method. Fig. 3 shows the results of the power coupling ratio as a function of the metal width w_2 with different metal thicknesses. In the range of small metal width w_2, the smaller metal width w_2 can lead to the smaller power coupling ratio because of the large mode mismatch resulting from the effects of the surface plasmon polaritons. In the range of large width w_2, such as 0.56 μm $\sim$ 0.8 μm, the power coupling ratio has a small variation around the value of 0.94. Besides, the impact of the metal thickness on the power coupling ratio can be basically negligible, especially in the range of large metal width w_2. But it should be noted that the metal thickness has an important influence in the mode conversion efficiency when the light is propagated in the hybrid plasmonic waveguide. Here the metal width w_2 is chosen as 0.7 μm. And the metal thickness should be further optimized next.

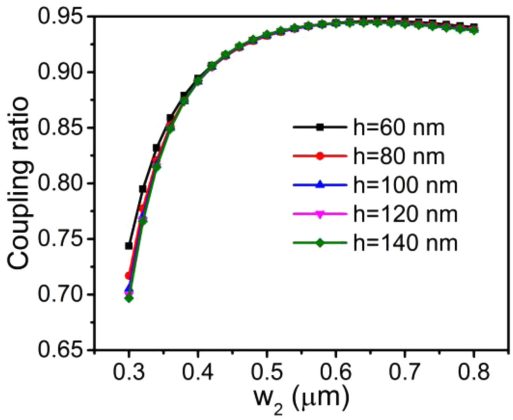

Fig. 3. The dependence of the power coupling ratio on the metal width w_2 with different metal thicknesses.

The tapered structure of the metal plays an important role on the mode conversion. To study the dependence of the mode conversion efficiency on the tapered structure, the transmissivity of the TM_1 mode and TE_0 mode with sweeping the metal width w_1 and the metal length L are demonstrated in Fig. 4(a) and (b). To evaluate the device performances of the proposed mode converter, the insertion loss and the extinction ratio are calculated in Fig. 4(c) and (d). Here the insertion loss (IL) and extinction ratio (ER) are defined as follows:

$$IL = -10 \times \lg(T_{total}) \tag{2}$$

$$ER = 10 \times \lg(T_{TM_1}) - 10 \times \lg(T_{TE_0}). \tag{3}$$

Where T_{total}, T_{TM1} and T_{TE0} are the transmissivity of the total input light, the TM_1 mode and the TE_0 mode in the output Si waveguide, respectively. In general, the larger metal width w_1 will lead to the smaller transmissivity of the TM_1 mode and the larger transmissivity of the TE_0 mode. In addition, the insertion loss is increased with the increasing of the metal length L. To obtain a high extinction ratio and a low insertion loss of the mode converter, the metal width w_1 and the metal length L are chosen as 0.16 μm and 11 μm, marking in Fig. 4(d), in which the extinction ratio is 24.1 dB and the insertion loss is 4.0 dB. Although there are some areas that the extinction ratio is larger than 24.1 dB, the insertion loss is also much larger than 4.0 dB which indicates a very low transmissivity of the input light. Besides, the metal length is also up to 20 μm and the large footprint is bad for the integration.

Fig. 5 displays the transmissivity of the TM_1 mode and TE_0 mode with different metal thicknesses. The impact of the metal thickness on the transmissivity of the TM_1 mode can be negligible. However, the transmissivity of the TE_0 mode is first decreased and then increased with the increasing the metal thickness. Here, the metal thickness is chosen as 70 nm which the transmissivity of the TE_0 mode is -39.5 dB and the extinction ratio is up to 35.1 dB.

3. Results and Discussions

Fig. 6(a) displays the spectral response of the transmissivity of the TM_1 mode and TE_0 mode in the output Si waveguide when the TE_0 mode is launched from the forward direction. The calculated wavelength range is from 1.46 μm to 1.625 μm covering the whole S, C and L band. An ultra-wide operation bandwidth from 1.5 μm to 1.6 μm is achieved with the extinction ratio larger than 20 dB. Moreover, at the wavelength of 1.55 μm, the transmissivity of the TM_1 mode is -4.4 dB and that of the TE_0 mode is -39.5 dB. The total insertion loss is only 4.2 dB. These results indicate that the proposed mode converter has good performances in mode conversion from TE_0 mode to TM_1

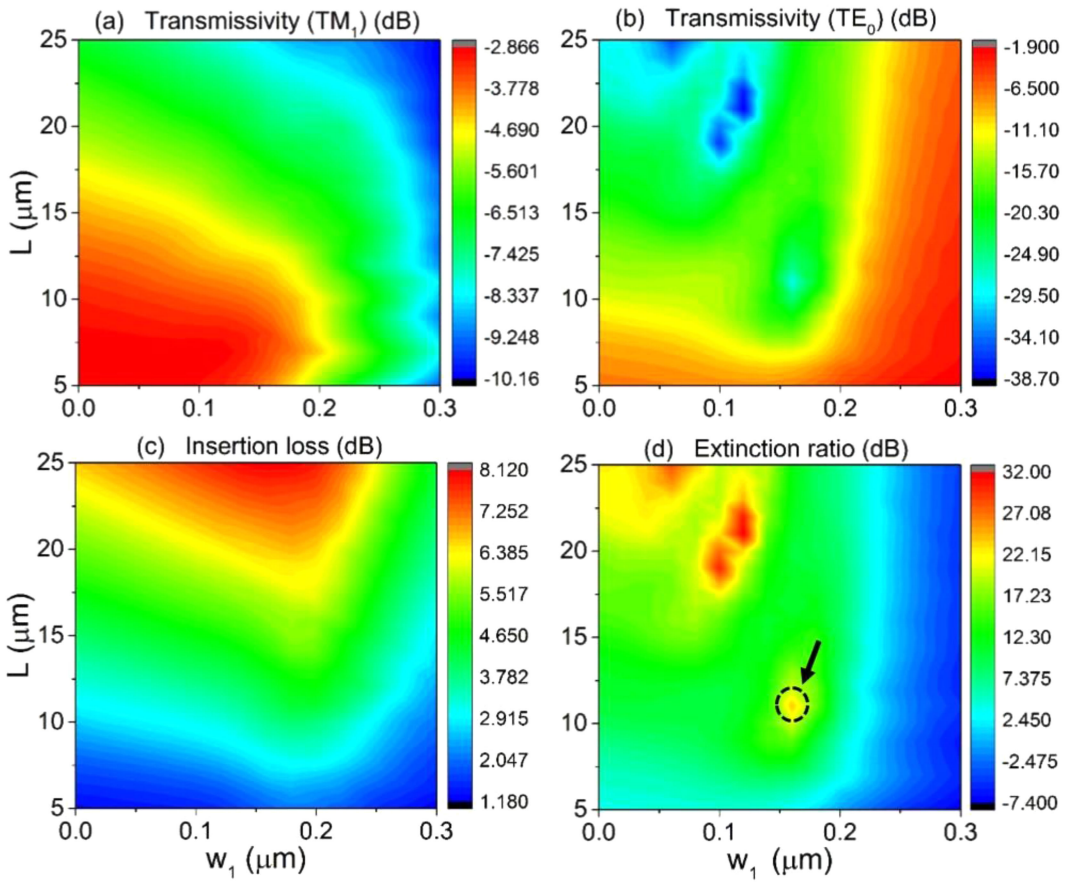

Fig. 4. The transmissivity of the mode converter with sweeping the metal width w_1 and the metal length L for (a) the TM_1 mode and (b) the TE_0 mode. (c) The insertion loss of the mode converter. (d) The extinction ratio between the TE_0 mode and TM_1 mode in the output waveguide.

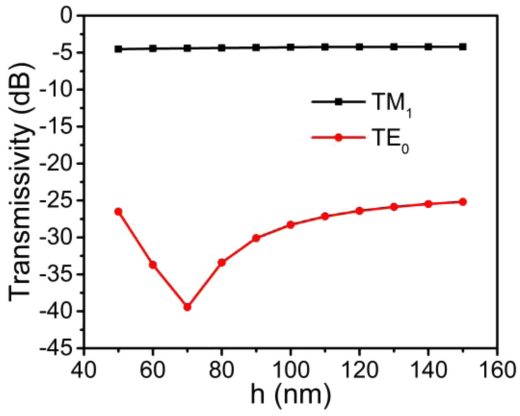

Fig. 5. The transmissivity of the TM_1 mode and TE_0 mode with different metal thicknesses h.

mode. Considering the back-propagation of the light, the spectral response is also calculated when the TM_1 mode is launched from the back direction and converted into the TE_0 mode, shown as in Fig. 6(b). It can be found that an operation bandwidth from 1.47 μm to 1.535 μm is also achieved with the extinction ratio larger than 20 dB. But the position of the peak value of the extinction ratio is obviously deviated from 1.55 μm. At the wavelength of 1.55 μm, the transmissivity of the TM_1

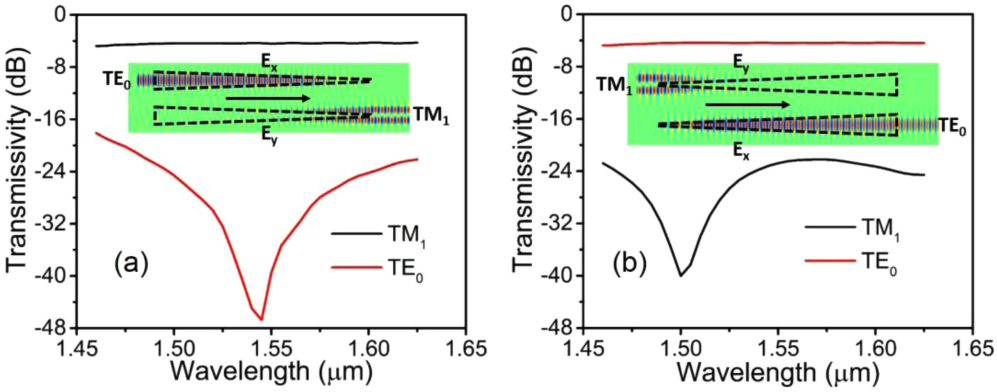

Fig. 6. (a) The spectral response of the transmissivity of the TM_1 mode and TE_0 mode when the TE_0 mode is launched from the forward direction. (b) The spectral response of the transmissivity of the TM_1 mode and TE_0 mode when the TM_1 mode is launched from the back direction.

TABLE 1
Comparison of Various Mode Converters

		Function	Length (μm)	Insertion loss (dB)	Bandwidth (nm)
Our work	Tapered hybrid plasmonic waveguide	TE_0-to-TM_1	11	4.2	100 (ER>20 dB)
[22]	Tapered waveguide with angled sidewalls	TM_0-to-TE_1	>200	Conversion efficiency $\approx$ 100%	
[27]	Bilevle taper	TM_0-to-TE_1	9	Conversion efficiency > 97%	
[18]	Metasurface	TE_0-to-TE_1	5.75	<1	21 (ER>10 dB)
[28]	Periodically perturbed waveguide	TE_0-to-TE_1	12	<0.5	23 (ER>20 dB)

mode is -22.8 dB and that of the TE_0 mode is -4.4 dB. The total insertion loss is only 4.1 dB. The insets of Fig. 5(a) and (b) are the electric field component distributions in the hybrid plasmonic waveguide at the wavelength of 1.55 μm when the light is launched from the forward direction and back direction. It clearly demonstrates the process of the mode conversion. A comparison of various mode converters with different structures has been demonstrated in Table 1. According to Table 1, the main disadvantage of our proposed mode converter is the large insertion loss due to the absorption loss of the metal, the main advantage of our mode converter is the wide bandwidth and the function of realizing the mode conversion from the TE_0 mode to the TM_1 mode.

The structure parameters of the metal have an important impact on the device performances. Considering the fabrication errors, the tolerance analysis on the transmissivity of the TM_1 mode and TE_0 mode is demonstrated when the TE_0 mode is launched from the forward direction, shown as in Fig. 7. On the whole, the impact of the fabrication errors on the transmissivity of the TM_1 mode can be negligible. The main source of the device performances degradation is the deviation of the metal width w_1. And the transmissivity of the TE_0 mode with other parameters deviation almost keeps in stable. In Fig. 7(b), at the wavelength of 1.55 μm, the transmissivity of the TE_0 mode is even getting smaller with a $+10$ nm deviation of the metal width w_2 which indicates the device performances are getting better. The results show that the device performances can be further improved by balancing the power coupling ratio and the transmissivity of the TE_0 mode. In Fig. 7(d), considering the difficulty in accurate controlling the device length in the fabrication process, the transmissivity of the TM_1 mode and TE_0 mode with a ± 50 nm deviation of the metal length L is

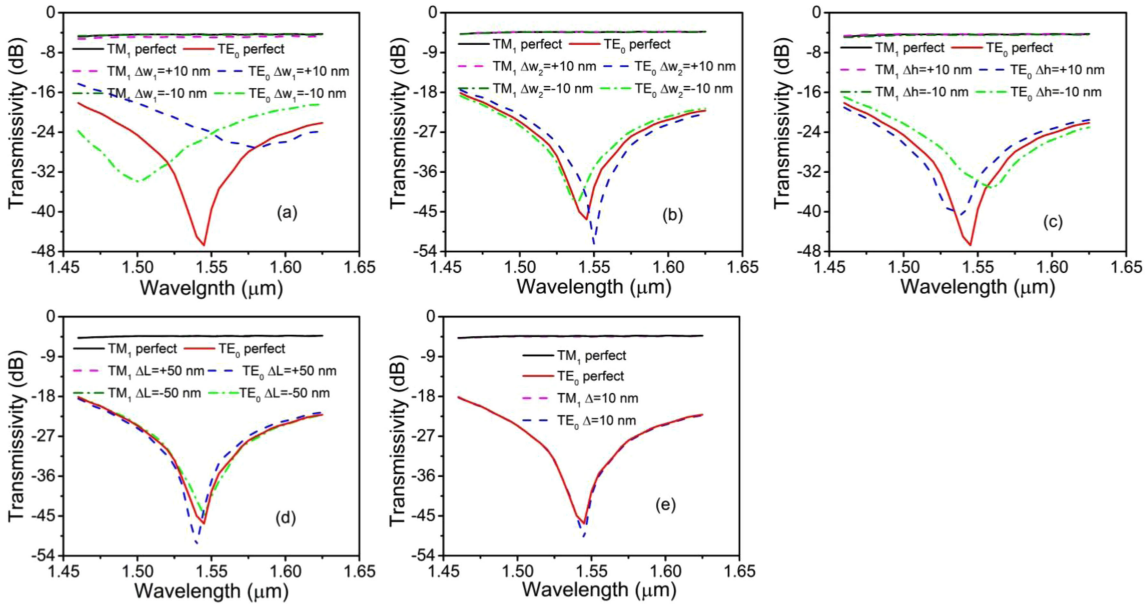

Fig. 7. Tolerance analysis of the mode converter with (a) a ±10 nm deviation of the metal width w_1, (b) a ±10 nm deviation of the metal width w_2, (c) a ±10 nm deviation of the metal thickness h, (d) a ±50 nm deviation of the metal length L and (e) a 10 nm deviation from the center of the waveguide.

calculated. For the transmissivity of the TE_0 mode with a +50 nm deviation, the position of the peak value is blue shifted and the peak value is getting smaller. It indicates the peak value of the extinction ratio can be further improved. In Fig. 7(e), the impact of the deviation from the center of the waveguide is also considered. It should be noted that the +10 nm deviation and the −10 nm deviation is the same due to the symmetry of the waveguide.

4. Conclusions

In summary, we have demonstrated a mode converter to achieve the mode conversion between the TE_0 mode and TM_1 mode by using the tapered hybrid plasmonic waveguide. With only 11 μm device length, an ultra-wide operation bandwidth of 100 nm is obtained with the extinction ratio of the TM_1 mode and TE_0 mode larger than 20 dB for the TE_0-to-TM_1 conversion. And for the TM_1-to-TE_0 conversion, when the light is input in the back direction, the operation bandwidth over 65 nm is obtained with the extinction ratio larger than 20 dB. The fabrication tolerance analysis also shows the mode converter has an acceptable fabrication error robustness. Although the waveguide with the thickness of 340 nm is used to analyze, waveguides with other thicknesses can also be applied in the mode converter. But the structure parameters should be re-optimized individually. In addition, other metals, such as Ag, can also be used. The deficiency of the mode converter is the relatively large insertion loss due to use the hybrid plasmonic waveguide without a thin low-index layer. We hope the mode converter can promote the development in the on-chip MDM systems of the PICs.

References

[1] W. Bogaerts and L. Chrostowski, "Silicon photonics circuit design: Methods, tools and challenges," *Laser Photon. Rev.*, vol. 12, no. 4, pp. 17002371–170023729, 2018.
[2] Q. Cheng *et al.*, "Recent advances in optical technologies for data centers: A review," *Optica*, vol. 5, no. 11, pp. 1354–1370, 2018.

[3] A. H. Atabaki *et al.*, "Integrating photonics with silicon nanoelectronics for the next generation of systems on a chip," *Nature*, vol. 556, no. 7701, pp. 349–354, 2018.
[4] L. W. Luo *et al.*, "WDM-compatible mode-division multiplexing on a silicon chip," *Nature Commun.*, vol. 5, 2014, Art. no. 3069.
[5] B. Stern *et al.*, "On-chip mode-division multiplexing switch," *Optica*, vol. 2, no. 6, pp. 530–535, 2015.
[6] D. Ohana and U. Levy, "Mode conversion based on dielectric metamaterial in silicon," *Opt. Exp.*, vol. 22, no. 22, pp. 27617–27631, 2014.
[7] H. Xu and Y. Shi, "Subwavelength-grating-assisted silicon polarization rotator covering all optical communication bands," *Opt. Exp.*, vol. 27, no. 4, pp. 5588–5597, 2019.
[8] A. Majumder, B. Shen, R. Polson, and R. Menon, "Ultra-compact polarization rotation in integrated silicon photonics using digital metamaterials," *Opt. Exp.*, vol. 25, no. 17, pp. 19721–19731, 2017.
[9] L. Chen, C. R. Doerr, and Y. K. Chen, "Compact polarization rotator on silicon for polarization-diversified circuits," *Opt. Lett.*, vol. 36, no. 4, pp. 469–471, 2011.
[10] D. Dai, "Advanced passive silicon photonic devices with asymmetric waveguide," *Proc. IEEE*, vol. 106, no. 12, pp. 2117–2143, Dec. 2018.
[11] L. Liu, Y. Ding, K. Yvind, and J. M. Hvam, "Efficient and compact TE–TM polarization converter built on silicon-on-insulator platform with a simple fabrication process," *Opt. Lett.*, vol. 36, no. 7, pp. 1059–1061, 2011.
[12] B. Bai, L. Liu, and Z. Zhou, "Ultracompact, high extinction ratio polarization beam splitter-rotator based on hybrid plasmonic-dielectric directional coupling," *Opt. Lett.*, vol. 42, no. 22, pp. 4752–4755, 2017.
[13] J. Zhang, S. Zhu, H. Zhang, S. Chen, G. Q. Lo, and D. L. Kwong, "An ultracompact surface plasmon polariton-effect-based polarization rotator," *IEEE Photon. Technol. Lett.*, vol. 23, no. 21, pp. 1606–1608, Nov. 2011.
[14] Y. J. Chang and R. W. Feng, "Embedded-silicon-strip-to-hybrid-plasmonic waveguide polarization mode converter," *IEEE Photon. Technol. Lett.*, vol. 29, no. 9, pp. 759–762, May 2017.
[15] D. Zhu, H. Ye, Z. Yu, J. Li, F. Yu, and Y. Liu, "Design of compact TE-polarized mode-order converter in silicon waveguide with high refractive index material," *IEEE Photon. J.*, vol. 10, no. 6, Dec. 2018, Art. no. 2883209.
[16] D. Chen, X. Xiao, L. Wang, Y. Yu, W. Liu, and Q. Yang, "Low-loss and fabrication tolerant silicon mode-order converters based on novel compact tapers," *Opt. Exp.*, vol. 23, no. 9, pp. 11152–11159, 2015.
[17] D. Ohana, B. Desiatov, N. Mazurski, and U. Levy, "Dielectric metasurface as a platform for spatial mode conversion in nanoscale waveguides," *Nano Lett.*, vol. 16, no. 12, pp. 7956–7961, 2016.
[18] H. Wang, Y. Zhang, Y. He, Q. Zhu, L. Sun, and Y. Su, "Compact silicon waveguide mode converter employing dielectric metasurface structure," *Adv. Opt. Mater.*, vol. 7, no. 4, pp. 1801191–1801196, 2019.
[19] V. Liu, D. A. B. Miller, and S. H. Fan, "Ultra-compact photonic crystal waveguide spatial mode converter and its connection to the optical diode effect," *Opt. Exp.*, vol. 20, no. 27, pp. 28388–28397, 2012.
[20] Y. Huang, G. Xu, and S. T. Ho, "An ultracompact optical mode order converter," *IEEE Photon. Technol. Lett.*, vol. 18, no. 21, pp. 2281–2283, Nov. 2006.
[21] H. Guan *et al.*, "Ultracompact silicon-on-insulator polarization rotator for polarization-diversified circuits," *Opt. Lett.*, vol. 39, no. 16, pp. 4703–4706, 2014.
[22] D. Dai and M. Zhang, "Mode hybridization and conversion in silicon-on-insulator nanowires with angled sidewalls," *Opt. Exp.*, vol. 23, no. 25, pp. 32452–32464, 2015.
[23] D. Dai, Y. Tang, and J. E. Bowers, "Mode conversion in tapered submicron silicon ridge optical waveguides," *Opt. Exp.*, vol. 20, no. 12, pp. 13425–13439, 2012.
[24] D. Dai and J. E. Bowers, "Novel concept for ultracompact polarization splitter-rotator based on silicon nanowires," *Opt. Exp.*, vol. 19, no. 11, pp. 10940–10949, 2011.
[25] 2019. [Online]. Available: https://www.filmetrics.com/refractive-index-database
[26] A. W. Snyder and J. D. Love, *Optical Waveguide Theory*. Berlin, Germany: Springer Science & Business Media, 2012.
[27] H. Guan *et al.*, "Ultracompact silicon-on-insulator polarization rotator for polarization-diversified circuits," *Opt. Lett.*, vol. 39, no. 16, pp. 4703–4706, 2014.
[28] P. G. Diego *et al.*, "Mode converters based on periodically perturbed waveguides for mode division multiplexing," *Proc. SPIE*, vol. 10686, 2018, Art. no. 106860R.